Preprints.org

Article

Assessing the Differentiation Capacity of Human Lung Fibroblasts towards Endothelial Cells for Potential Clinical Exploitation

Nikoleta F. Theodoroula , Alexandros Giannopoulos-Dimitriou , Aikaterini Saiti ,

Aliki Papadimitriou-Tsantarliotou , Yiannis Sarigiannis , Dimitrios G. Fatouros , Ioannis S. Vizirianakis [*]

Article

Assessing the Differentiation Capacity of Human Lung Fibroblasts towards Endothelial Cells for Potential Clinical Exploitation

Nikoleta F. Theodoroula [1], Alexandros Giannopoulos-Dimitriou [1], Aikaterini Saiti [1], Aliki Papadimitriou-Tsantarliotou [1], Yiannis Sarigiannis [2], Dimitrios G. Fatouros [3] and Ioannis S. Vizirianakis [1,2,*]

[1] Laboratory of Pharmacology, School of Pharmacy, Aristotle University of Thessaloniki, Thessaloniki 54124, Greece; theodorn@pharm.auth.gr (N.F.T.); gianalex@auth.gr (A.G-D.); skaikater@auth.gr (A.K.); alikipapadi@pharm.auth.gr (A.P-T.); ivizir@pharm.auth.gr (I.S.V.)

[2] Department Health Sciences, School of Life & Health Sciences, University of Nicosia, Nicosia 2417, Cyprus; sarigiannis.i@unic.ac.cy (Y.S.); vizirianakis.i@unic.ac.cy (I.S.V.)

[3] Department of Pharmaceutical Technology, School of Pharmacy, Aristotle University of Thessaloniki, Thessaloniki 54124, Greece; dfatouro@pharm.auth.gr (D.G.F.)

* Correspondence: ivizir@pharm.auth.gr (I.S.V.).

Abstract: The role of mesenchymal-to-endothelial transition in the angiogenic response is controversial. Toward this, the present study aimed to determine if fibroblasts contribute to angiogenesis. Endothelial differentiation of fibroblasts was induced by culturing MRC-5 cells (human fetal lung fibroblast cells) on top of Matrigel hydrogel or embedded inside the hydrogel. The formation of capillary-like networks in response to angiogenic signals was observed. The tube formation occurs quickly and can be visualized using a phase-contrast inverted microscope, and/or the cells can be treated with DAPI before the assay and tubes can be visualized through fluorescence or confocal microscopy. Furthermore, fibroblasts cultured in a higher concentration invaded the Matrigel hydrogel and formed stem-cell-like spheroids. These spheroids embedded in matrigel matrices of varying densities sprouted to form 3D connective-tissue networks. Collectively, our results highlight the endothelial differentiation capacity of human lung fibroblasts. The results obtained in this work may have an impact on the search for alternative cell sources for vascular tissue engineering and the overcome of obstacles to vascularization of autologous tissue-engineered constructs and the production of functional grafts for clinical use.

Keywords: fibroblasts; endothelial cell; differentiation; tissue engineering; matrigel

1. Introduction

New blood vessels formation by endothelial cells (ECs) is of great importance to clinicians and researchers as it has significant potential to make a major impact on the treatment of cardiovascular disease. Tissue engineering has emerged as a promising approach to the creation of a bio-compatible vessel graft with the ability to grow, remodel, and repair *in vivo*. Considerable advancements in the area of vessel engineering have been reported [1–4]since Weinberg and Bell, in 1986, succeeded in creating for the first time a blood vessel from collagen, endothelial cells, smooth muscle cells, and fibroblasts.[5] However, after a few decades of research, despite the considerable progress in the field of vascular tissue engineering still numerous difficulties remain. The major issues include considerable technical obstacles to acquiring autologous ECs for injury treatment and tissue engineering due to the limited source, harvest procedure, and proliferative capacity of these cells.[6–8] However, some of these difficulties in vascular tissue engineering can be overcome by the use of endothelial progenitor cells (EPCs).[9] This subtype of stem cells have the potent capacity to proliferate *in vitro* and differentiate into mature ECs.[10] In addition, there are multipotent stromal cells (MSCs) that can differentiate into a variety of lineages.[11] However, the clinical use of MSCs and EPCs has also been limited due to difficulties associated with their harvest, culture, and

expansion.[12–14] Thus, the demand for an alternative cell source to develop a suitable method for obtaining abundant human ECs *in vitro,* for the formation of new blood vessels, continues to grow.

Fibroblasts are traditionally defined as diverse mesenchymal cells that participate in tissue homeostasis and disease. They are involved in the formation, maintenance, and degradation of the extracellular matrix (ECM), thereby contributing to the mechanical properties of tissues.[15,16] It is therefore not surprising that fibroblasts have been suggested to contribute to angiogenesis through modulation of the ECM network and protein secretion, crucial for lumen formation and EC sprouting.[17] These angiogenic mediators include vascular endothelial growth factor [18] and angiogenic chemokines. Whether fibroblasts directly contribute to angiogenesis by converting to endothelial cells through mesenchymal to endothelial transition (MEndoT) needs to be further investigated. Transdifferentiation of fibroblasts to endothelial cells (ECs) may provide a novel therapeutic avenue for cardiovascular diseases. Recently, several studies have demonstrated that fibroblasts may be reprogrammed into ECs in vitro.[19–25]

The present study further evaluates the endothelial differentiation capacity of MRC-5 lung fibroblasts. In this paper, we describe a unique method of direct conversion of lung fibroblasts into ECs, exhibiting endothelial morphology and endothelial functions similar to those of authentic, functional ECs. By growing MRC-5 cells on top of Matrigel hydrogel, the differentiated ECs exhibited the capability to form capillary structure within 24hrs, or EC sprouts when being embedded in the matrix. Our findings suggest a novel strategy that offers an alternative approach to overcoming challenges in acquiring autologous ECs.

2. Materials and Methods

2.1. Hydrogel

Matrigel hydrogel was used to study the phenotypes of human lung fibroblast MRC-5 cells grown on top of the matrices or embedded**.** Matrigel (Corning, NYC, NY, USA) consists of basal membrane extract derived from Engelbreth-Holm-Swarm mouse sarcoma cells. At room temperature, it solidifies and forms a hydrogel. The extracellular matrix components present in this hydrogel include laminin, collagen IV, entactin, nidogen, and heparan sulphate proteoglycans. Growth factors such as TGF-β, basic fibroblast growth factor, insulin-like growth factor-1, and tissue plasminogen activator are also present. Matrigel has previously been used and has been shown to stimulate *in vitro*.

2.2. Cell cultures and treatments

The already established human normal MRC-5 (fetal lung fibroblasts) are stored and routinely used in our laboratory. The MRC-5 cells were grown in culture (37°C; humidified atmosphere containing 5% *v/v* CO_2) in 25 cm^2 flasks and/or in a 6 or 96-multiwell microplate, according to the type of assay to be performed, in 1× Dulbecco's modification of Eagle's medium (DMEM, Corning) supplemented with 10% (v/v) fetal bovine serum (FBS) and 1% penicillin/streptomycin (Gibco). The treatments were performed at sub-confluence and then the cells were detached by using trypsin-EDTA (0.25% w/v, Life Technologies).[26]

The human umbilical vein endothelial cell line (HUVEC cells) were grown in Endothelial Cell Culture Medium (Sigma-Aldrich, Merck KGaA, Darmstadt, Germany), as previously published [27].

2.3. Tube Formation Assay

The *in vitro* tube formation assay on Corning® Matrigel® Matrix (Corning, NYC, NY, USA) was conducted according to a previously published protocol.[28] Following a slow overnight thawing on the ice at 4°C of Corning Matrigel Matrix, according to the recommendations provided in the product Guidelines for Use, 250 μL of matrigel solution was dispensed into each well of a 24-well plate and incubated for 30 min at 37 °C, for the experiment of MRC-5 and HUVEC cells grown on Matrigel. Cell suspensions were prepared by trypsinizing the cell monolayers with trypsin–EDTA and

resuspending the cells in culture medium of 10% FBS. 500 µL of cells were seeded on the top of Matrigel 10 mg/mL at a starting density of 10^5 cells/mL, 1.5×10^5 cells/mL, or 3×10^5 cells/mL respectively, at 37 °C. The matrix-coated well plates were incubated for 24 h for cell tube formation. After being incubated for 24 hours at 37 °C, images of tube formation were taken accordingly. Additional experiments were conducted to determine the optimal concentration, which allowed cells to show either an increase or decrease in tube formation ability. For experiments on tube formation, samples were photographed with magnifications x40, and x20 magnification using an inverse light microscope. Each experiment was repeated at least three times independently.

2.4. Quantitative ImageJ Analysis for Angiogenic Assay

The ImageJ software (Wayne Rasband, National Institute of Health, Bethesda, MD, USA) was used by applying the "Angiogenesis Analyzer" plug-in tool to analyze several different parameters related to the tube formation as described in the Results section. Indicators of the analyzed tube forming elements included the number of junctions, segments, meshes, etc. The ImageJ plug-in, "Angiogenesis Analyzer," was used to quantitatively evaluate the vessel-like network organization. "Segments" indicate the portions of an angiogenic capillary with two ends connected to two junction points "Junctions" are the multi-intersection junctions with furcates of three or more branches in the angiogenic structures. "Meshes" represent closed areas formed by segments.

2.5. Fluorescent Staining

After 24hrs of incubation, the cells were washed twice with PBS and fixed in Intracellular Staining Fixation Buffer (BioLegend, Cat. No. 420801) for 20 min. The cells were then rinsed with PBS and permeabilized with Intracellular Staining Permeabilization Wash Buffer 10X diluted to 1X in DI water (BioLegend, Cat. No.421002) for 10 min. The coverslips were mounted onto glass microscope slides in Prolong Gold Antifade Reagent with DAPI, sealed, and left overnight in the dark at 4 °C. The fluorescent signals of (DAPI)-labeled cell nuclei were imaged with a 40x oil-immersion lens under a Zeiss LSM 780 CLSM (Carl Zeiss Microscopy GmbH, Berlin, Germany) using appropriate filters.

2.6. Cell invasion assay

The Oris Universal Cell Migration Assembly kit was purchased from Platypus Technologies, LLC (Fitchburg, WI, USA). Each 96-well plate of the kit contained cell-seeding stoppers (2 mm in diameter) for creating a detection zone at the center of each well. The wells of the 96-well plate were coated with 50 µL/well of diluted Matrigel® (100µg/mL). The plate was placed in a 37° C incubator, 5% CO_2 to allow the biomatrix material to polymerize for 2 hours to study MRC-5 cell invasion. After 2 h the plate was removed from 37° C and Cell Seeding Stoppers were placed. One well without a Cell Seeding Stopper served as the positive control. MRC-5 cells (100 µL/well, 100,000–400,000 cells/mL stock) were seeded into each well of the plate. The seeded plate containing the Oris™ Cell Seeding Stoppers was incubated in a humidified chamber (37°C, 5% CO_2) overnight to permit cell attachment. After the cells were attached to the matrices the spacers were removed. Media was removed and wells were washed with 100 µL of sterile PBS. After washing, 100 µL of culture media was added, and the cell plate was cooled to 4° C for 5 min. The top layer of the matrix was prepared on ice by diluting Matrigel®, 4-8 mg/mL. 50µL of the Matrigel® top layer was added. The addition of the two Matrigel™ layers ensured that the assay measures invasion, as opposed to 2D wound healing migration. The cell plate was then placed at 37° C for the biomatrix top layer to polymerize. After 30 min, 100 µL/well of additional media was added to each well and the plate was incubated in a humidified chamber (37°C, 5% CO_2) to permit cell invasion. Cells were examined microscopically after 24, 48, and 72 h to monitor the progression of invasion. Three independent biological experiments were performed for statistical analysis using Student's t-test. The images that were taken, were quantitated by WimScratch (Wimasis Image Analysis).

2.7. In vitro cell viability assay

Cell counting kit-8 (CCK-8, Dojindo) was used to assess the viability of lung human fibroblasts both in a 2D monolayer dish culture and in 3D constructs on top of Matrigel Matrix 10 mg/mL. MRC-5 cells were cultured in DMEM containing 1% penicillin-streptomycin solution and 10% FBS at 37 °C in 5% CO_2 condition. Five independent biological experiments were made for the measurement of cell viability and all data presented are the average from triplicate experiments. After 48 h of incubation, the Cell Counting Kit-8 (CCK8, Sigma- Aldrich) reagent was added to each well and the cells were incubated for 2 h at 37 °C. One hundred microliters of the supernatant were transferred into a 96-well plate and the OD was assessed at 450 nm in a multifunction microplate reader. Wells containing only the CCK-8 reagent were used as blank control.

Fluorescent dead staining was used to determine dead cells in the 3D cell-laden constructs according to the manufacturer's instructions. Briefly, samples were gently washed in PBS three times. Propidium Iodide (PI, 421301, BioLegend, San Diego, CA, USA) was used to stain dead cells (red) for 30 min in a cell incubator. A fluorescence imaging system (EVOS FL imaging system, AMF4300, Life Technologies) was used for observation and image acquisition. Death percentage was counted by Image-J software. Four random fields were counted for each sample.

2.8. RNA extraction and Real-Time Polymerase Chain Reaction (qPCR)

MRC-5 cells were plated on top of Matrigel Matrix gel. After treatment for 48hrs, total RNA was isolated from 3D Cell Cultures on top of Matrigel® Matrix 10mg/mL using the ReliaPrep™ miRNA Cell and Tissue Miniprep System (Z6211, Promega, Southampton, UK) according to the product protocol.[29] After isolation, RNA was tested qualitatively and quantitatively, respectively, by gel electrophoresis assay and by the means of NanoDrop 2000 (Thermo Fisher Scientific, Waltham, Massachusetts, USA) spectrophotometer. RNA samples were subjected to reverse transcription using the PrimeScript™ RT-PCR Kit (RR014A, Takara Bio Inc., Tokyo, Japan), as per the manufacturer's instructions. Quantitative RT-PCR analysis was performed using the KAPA SYBR FAST qPCR Kit (KK4602, Kapa Biosystems, Wilmington, MA, USA). The primer sequences of the genes related to cell cycle and proliferation are presented in Supplemental Table S1. The primer sequences of the endothelial biomarker genes used in qPCR analysis are shown in Supplemental Table S2.

2.9. Statistical Analysis

Data are presented as mean ± standard deviation (SD) of triplicate incubations. The student's t-test and one-way analysis of variance (ANOVA) were employed to evaluate the data. The significance level was set at $p \leq 0.05$.

3. Results.

3.1.O. ptimal cell number for tube formation assay

To evaluate the ability to undergo angiogenesis, the tube formation experiment is the key method used *in vitro*. We first tested whether MRC-5 cells can form tube-like networks on the three-dimensional Matrigel matrix and next we determined the optimal starting cell density needed to establish "vascular mimicry meshwork" *in vitro*. For this purpose, cells were seeded on Matrigel using different starting cell density of **10^5 cells/mL, 1.5×10^5 cells/mL, or 3×10^5 cells/mL respectively.** Interestingly, cell number has a profound impact on tube formation. MRC-5 cells formed well-defined, distinct interconnected tube-like structures when the seeding concentration was **1.5×10^5 cells/mL** (Figure 1A-C). This 'vessel-like' network resembles the early stages of endothelial cell tubulogenesis. When cultured under the same conditions but in a lower seeding density (**10^5 cells/mL)**, MRC-5 cells failed to form any consistent structures, and only small branches but no tubes were reported, because of the insufficient number of cells seeded on the matrix. As the number of seeded cells increases, the network of tubes expands. However, at higher concentrations (**3×10^5 cells/mL)**, the cells begin to invade the Matrigel matrix and form aggregates.

10^5 cells/mL   1.5 x 10^5 cells/mL   3 x 10^5 cells/mL

A   B   C
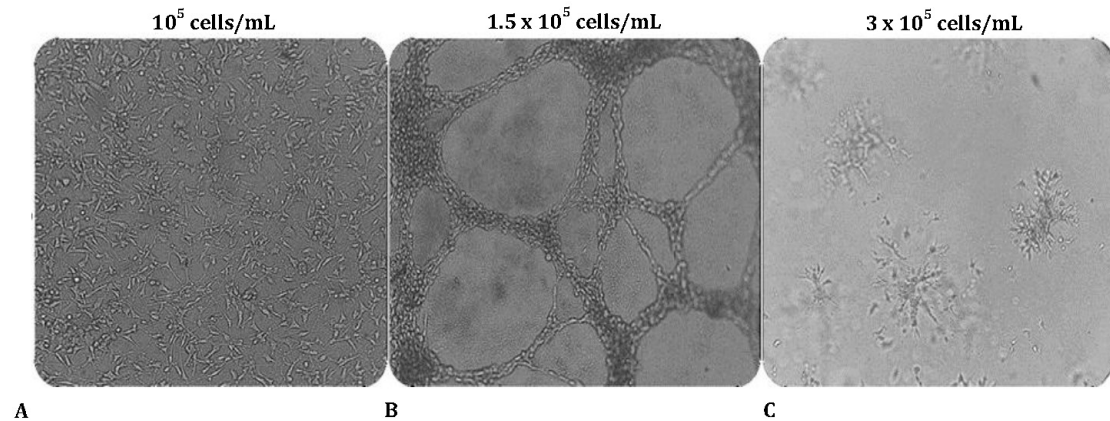
Figure 1. The effect of cell number density on MRC-5 tubulogenesis cultured on Matrigel. MRC-5 cells were seeded in wells at various cell concentrations shown above the panels (A-C). Note the capillary tube-like structures formed in panel B.

3.2. In vitro tube formation reveals different morphological patterns

To further assess the morphological pattern of MRC-5 cells seeded on Matrigel matrix in various starting densities, using 3 dimensional (3D) images, we utilized a confocal laser scanning microscope. The samples were stained with DAPI to label the nuclei of the MRC-5 cells as described in the Materials and Methods section. Interestingly, cells showed distinct morphological patterns of tubulogenesis *in vitro*. Specifically, alterations were detected when different starting concentrations of MRC-5 cells were seeded on top of the Matrigel matrix. The results obtained thus far confirmed that cell concentration affects the ability for tube formation (Figure 2A-C). Tubes were poorly formed when the starting cell seeding concentration was too low (**10^5 cells/mL),** confirming that this number of cells was not sufficient to initiate capillary structures in vitro. As more cells were seeded (**1.5×10^5 cells/mL)**, a tubal network was formed on top of matrigel and MRC-5 cells demonstrated a growth pattern similar to ECs after 24 h. However, when the cell concentration was raised to **3×10^5 cells/mL**, regular tube-like structure formation was not detected. In contrast, the cells became confluent, invaded Matrigel, and initiated the formation of sprouts originated by the previously formed spheroids embedded in the Matrigel.
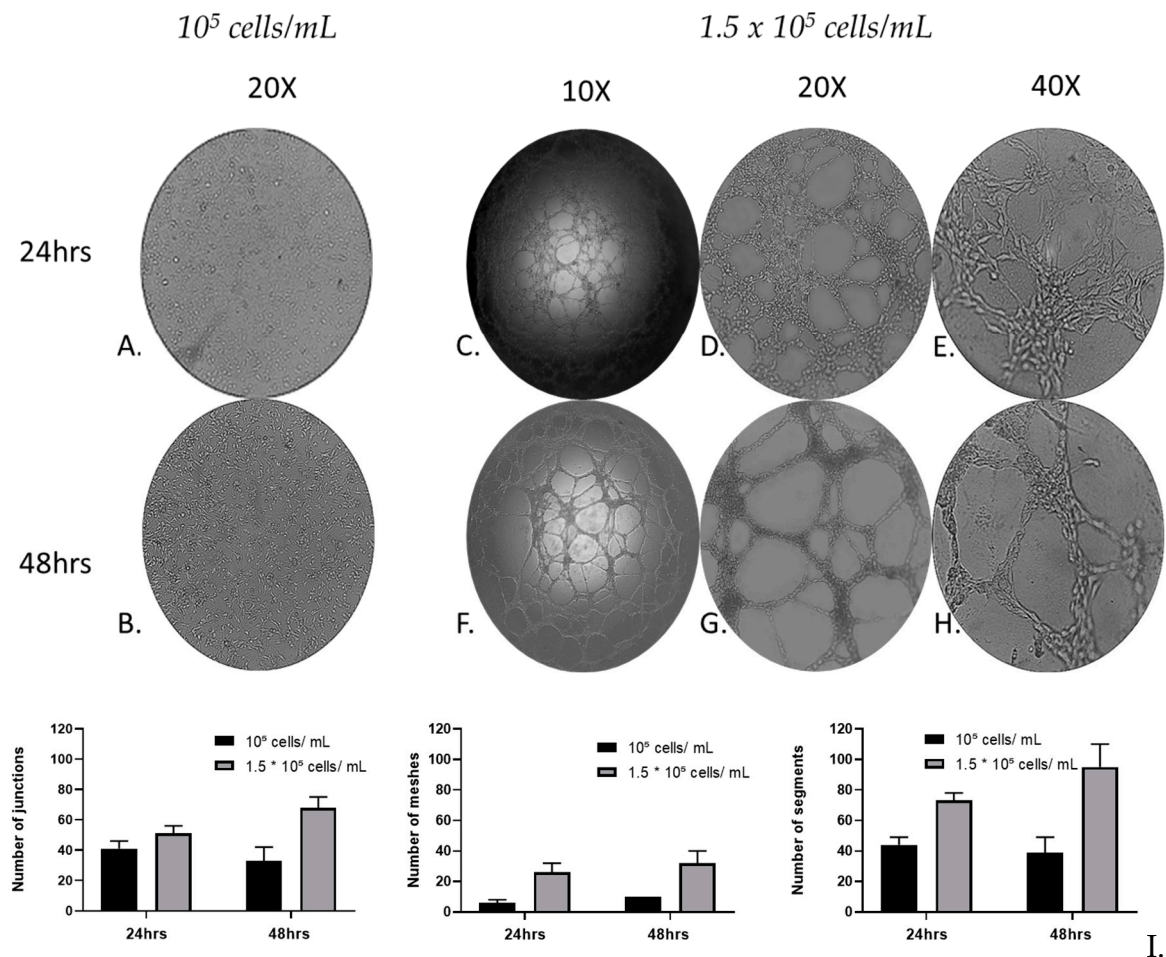
10^5 cells/mL   1.5 x 10^5 cells/mL   3 x 10^5 cells/mL

A   B   C
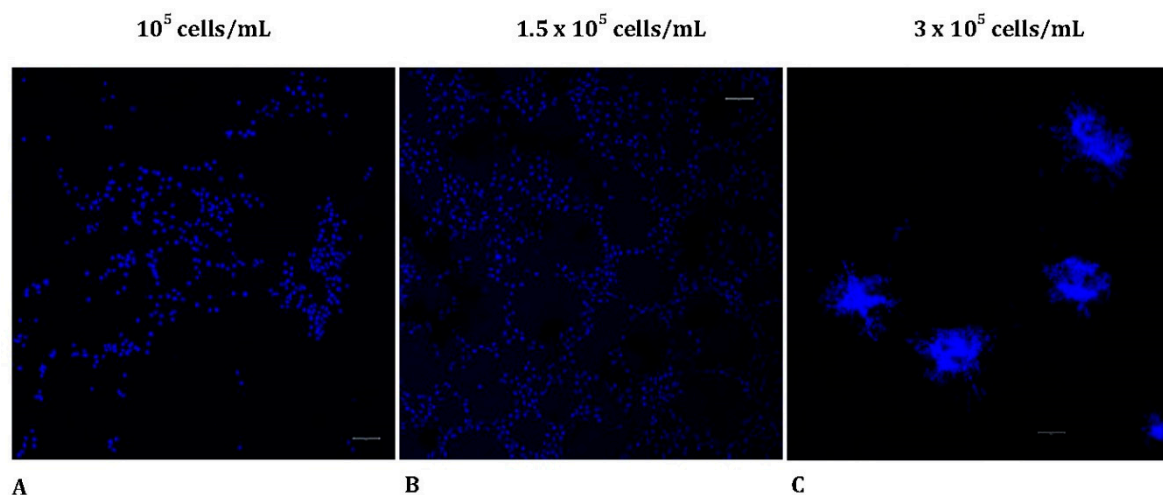
Figure 2. The morphological pattern in MRC-5 cultures seeded on Matrigel at various starting cell densities. (Scale bar = 20 μm). MRC-5 cells were incubated on Matrigel matrix and then fixed and stained with DAPI (blue), for visualizing the nuclei. Samples were visualized under CLSM. The different cell concentrations applied are shown above the panels (A-C). CLSM, confocal laser scanning microscopy; DAPI, 4',6-diamidino-2-phenylindole.

3.3. MRC-5 cell tube formation over time

To evaluate the cell tube formation of MRC-5 cells over time, a Matrigel-based tube-forming assay was employed for 48 h. Following the assay, representative images of the capillary-like tubular structures were taken and subsequent quantitative analysis, recording anastomotic network parameters, by utilizing the ImageJ Angiogenesis Analyzer tool [30]. The tube formation parameters analyzed, by using the Angiogenesis Analyzer plugin, include the number of junctions (branching capillary nodes), segments (capillaries delimited by two junctions), meshes (areas enclosed by segments).

After 24 and 48 h, the tube-forming assay (Figure 3C-H) revealed that the cultures of MRC-5 cells with starting seeding concentration of 1.5×10^5 cells/mL, formed a complex anastomosis network on the surface of Matrigel. Interestingly, although in these cultures a network of interconnected capillaries, complex and branched, was formed, in the cultures with starting seeding concentration of 10^5 cells/mL, cells didn't form capillary-like tubular structures (Figure 3A, B). Moreover, the capillary-like tubular structure was formed more densely, in a time-dependent manner; the complexity of the network formed by 48 h was higher than that of 24 h in terms of numbers of Junctions, Segments and Meshes. MRC-5 cells gradually formed capillary-like tubular structures, and the capillary-like tubes connected to each other created a mesh-like structure on the gel.

Figure 3. Qualitative and quantitative analysis of MRC-5 cell in vitro tube formation throughout 48hrs. MRC-5 lung fibroblast cells 10^5 cells/mL (A, B) and 1.5×10^5 cells/mL were incubated with Matrigel and the tube formation was recorded at 24 (A, C, D, E) and 48 h (B, F, G, H), respectively, under an inverted phase microscope. (I) Quantification of the capillary network by Angiogenesis Analyser plugin. A starting cell density of 1.5×10^5 cells/mL produced consistent mature looping patterns in Matrigel for at least 48 h. Data are representative of measures obtained from six to nine fields.

3.4. Cell viability and proliferation

The viability of human lung fibroblasts cultured on top of Matrigel reached 98.13% of control MRC-5 untreated cells, grown in plates without Matrigel, after 48 h and the death percentage was less than 4% eestimated by Image-J software. The results revealed that Matrigel Matrix hydrogel had no effect on the viability of MRC-5 cells. As shown in (Figure 3C-H), the capillary-like tubular structure was formed more densely and the tubular structures increased on day 2 (48h). In addition, the gene expression profiling, of three genes related to cell cycle and proliferation, when MRC-5 cells are seeded on top of Matrigel Matrix hydrogel 10mg/mL for 48 h does not reveal any major effects for two of the three genes tested. The three-cell cycle and proliferation-related genes that were tested with qPCR are Cdk2, Cdk6, and bcl-2. The reason for selecting only these three genes has been, that in previous work it was shown that only a limited number of proliferation- and apoptosis-related genes can be detected by molecular analysis in MRC-5 cells [26]. Although no significant differences were observed in the levels of Cdk6 and bcl-2 gene as compared with the untreated MRC-5 control cultures, the Cdk2 level was significantly decreased (Figure 4A). This decrease, however, in the gene expression profile of Cdk2 on day 2 (48hrs) implies an interruption in the regulation of the cell cycle, a fact that might contribute to proliferation restriction and facilitation of cell structure formation.
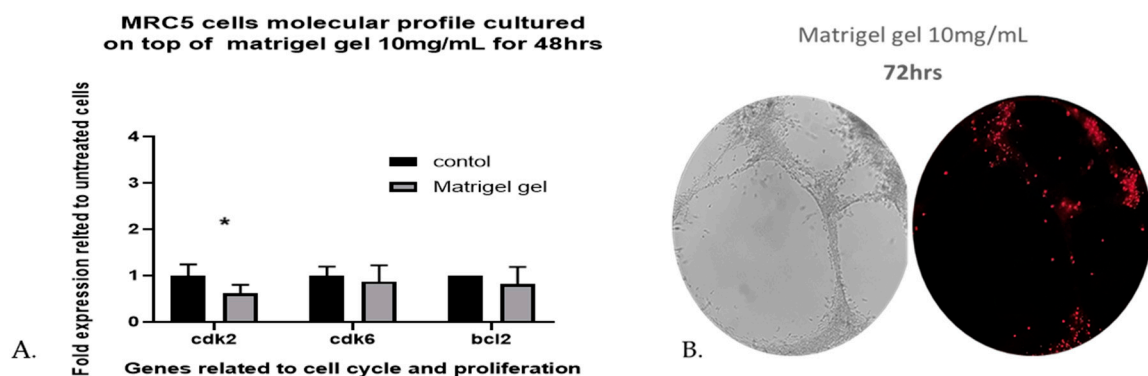
Figure 4. A. qPCR analysis of MRC-5 seeded on top of Matrigel Matrix gel 10mg/mL. The gene expression profiles for proliferation- and cell-cycle-related molecules in MRC-5 cells that had been cultured on top of Matrigel Matrix gel for 48 h in comparison to untreated MRC-5 control cultures, grown in plates without Matrigel, are presented. The analysis was carried out with qPCR with the primers shown in Supplementary Table S1, as described under Materials and Methods. The data shown above provide evidence of a representative experiment in which three measurements were made to calculate the mean (± SD). A biological replication of this experiment was carried out at least twice with similar results. Statistics were performed by paired t-test. A significance level of $p < 0.05$ denoted significance. **B. Propidium iodide (red) staining of human lung fibroblasts in Matrigel hydrogel constructs on day 3 (72 h).** Red spots indicate dead cells. The percentile of apoptotic of MRC-5 cells measured by Angiogenesis Analyser was 18.55%.

To further investigate the viability of MRC-5 cells remaining after 48 h, we used fluorescent dead staining, to determine dead cells in the 3D cell-laden constructs, according to the manufacturer's instructions. By 72 h, the estimated death percentage by Image-J software was 18.55% (Figure 4B), many branches remained, but many of the cells became apoptotic and some tubes began to disconnect.

3.5. Capillary sprouting from gel-embedded spheroids

When seeding MRC-5 cells at different densities on Matrigel gel 10mg/mL, we observed that beyond a critical density, cells invaded the matrix and formed aggregates. Cells originated from these formed 3D spheroids invaded through the gel and gave rise to radially outgrowing capillary sprouts which subsequently gave rise to complex anastomosing capillary-like networks (Figure 5A). Cells that were not integrated into the monolayer became apoptotic (Figure 5B). The spheroids embedded

in matrigel gel 10 mg/mL were cultured for at least 48 h after their formation. This observation prompted us to study more systematically MRC-5 sprouting in three-dimensional Matrigel matrix gel. Since cell adhesion is known to play an important role in the sprouting of cells in 3D matrices, we investigated the effects of the physical properties of the 3D matrix on cell sprouting patterns. We compared cell sprouting in the matrix as a function of matrix density obtained through two different matrigel concentrations from 5 and 10 mg/mL. As a result, we next extended our studies in an assay in which MRC-5 cells were seeded on Matrigel gel 5 mg/mL(Figure 5C). The outgrowth of these capillary-like structures was assessed qualitatively and quantitatively.
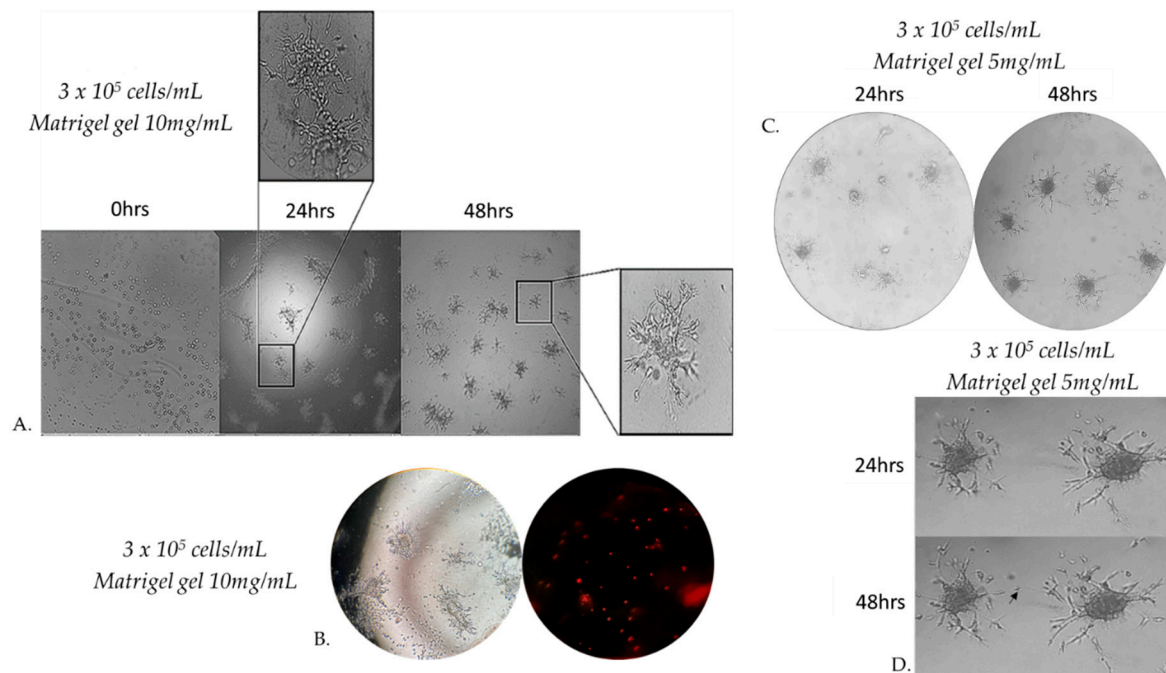
Figure 5. Morphology of capillary sprouts originating from MRC-5 cell spheroids embedded in 10 mg/mL Matrigel matrix gel. Note that gel-embedded spheroids give rise to radially outgrowing capillary sprouts. Outgrowing sprouts of neighbouring spheroids grow directionally towards each other to establish networks of anastomosing capillary-like structures, as shown by phase-contrast microscopic analysis **(A)**. Capillary-like structures of varying sizes form a true lumen throughout the gel. Cells that are not integrated into the monolayer become apoptotic **(B).** Directional sprouting of capillary-like structures towards each other, originating from two neighbouring spheroids, embedded in Matrigel gel 5 mg/mL. Capillary sprouts start to change their direction to grow towards each other **(C)**. Note that the centers of the two spheroids have moved closer together after 24 h **(D)**.

Within a few hours after the formation of the spheroids in matrigel gel 5 mg/mL, MRC-5 cells originating from the embedded spheroids progressively invaded the Matrigel matrix to form complex networks of capillary-like structures. Before 48 h, some sprouts changed their direction to grow towards a neighboring spheroid if this spheroid is in close proximity (Figure 5C,5D).

Embedded spheroids consist of two distinct populations: a migratory or invasive population and a non-migratory core. This is a consequence of the two distinct microenvironments present. Cell-matrix interactions dominate the invasive population and cell-cell contacts dominate the non-migratory core.[31] Initially, the spheroidal cells appeared as a compact structure, however, subsequent cell invasion caused spheroid expansion and resulted in breaches in the spheroid core. The spheroids were photographed after 48 h of incubation by a phase-contrast microscope. Sprout and spheroid area, on matrices of both densities, were quantitated by WimSprout (Wimasis Image Analysis). However, we didn't notice any significant difference between Matrigel gel 5mg/mL and 10mg/mL (Figure 6A–D).
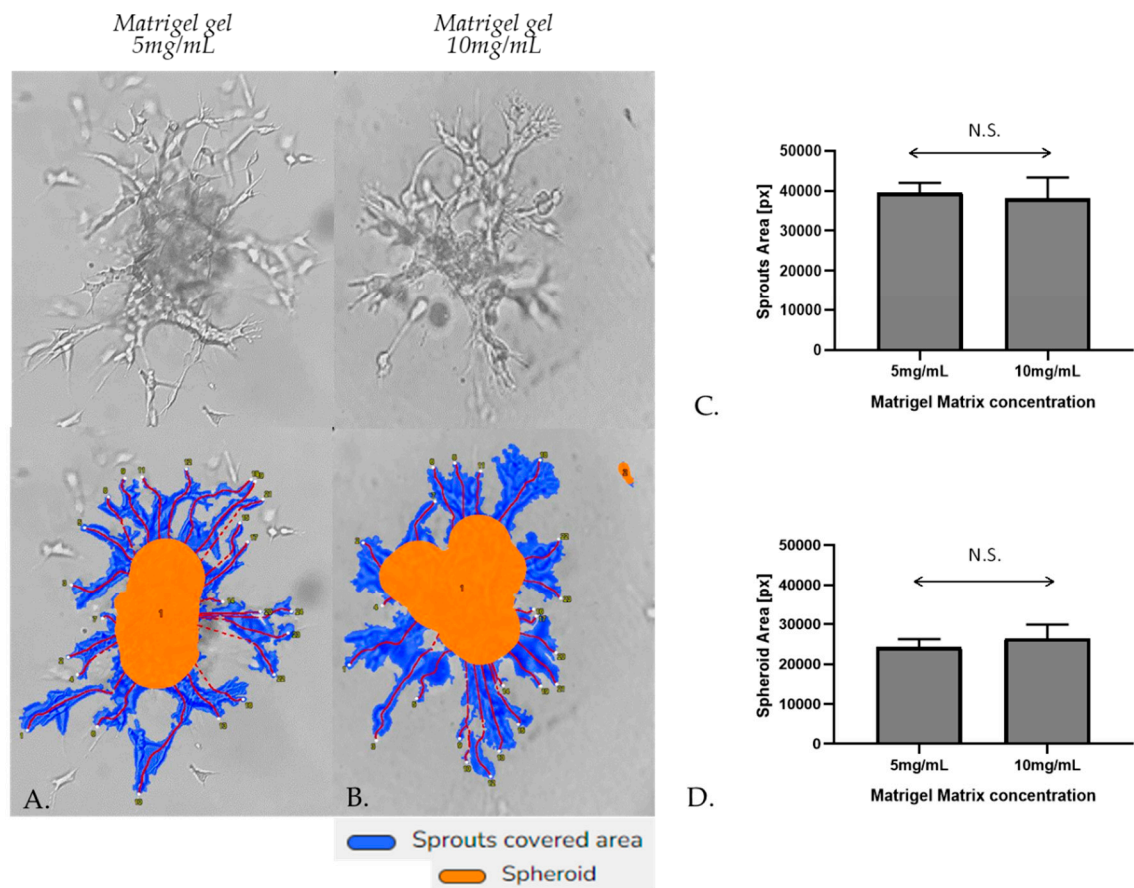
Figure 6. Representative sprouting morphology in Matrigel 5mg/mL (A) and Matrigel 10 mg/mL (B). Upper panel: Phase-contrast microscopic images of spheroids; Lower panel: Computer-processed images by WimSprout image analysis for sprouting determination. (N.S.: Not significant).

### 3.6. MRC-5 cells invade through Matrigel gel

To further examine and decouple the invasion capacities of MRC-5 cells on Matrigel matrix gel, we have utilized the Oris Universal Cell Migration Assembly kit as described in the Materials and Methods section. As we have observed, MRC-5 cells on Matrigel beyond a critical density invade through the gel. Photography and quantitative analysis of the results revealed that the invasion rate of cells cultured in semi-solid Matrigel increased in a time-dependent manner.
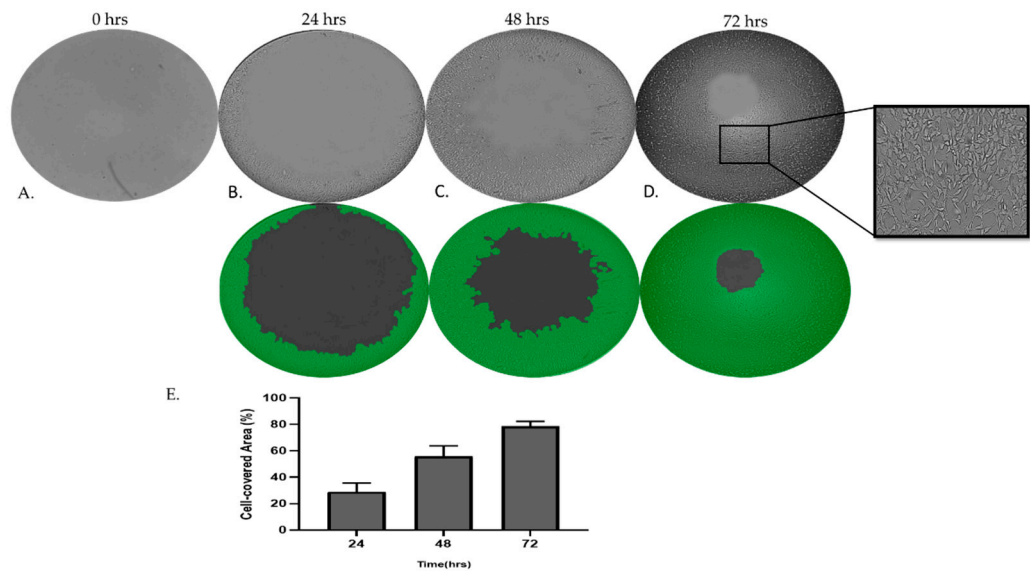
Figure 7. Assay for MRC-5 cell invasion through Matrigel™ using Oris Universal Cell Migration Assembly kit. MRC-5 cells were allowed to invade for 24 – 72 h through Matrigel® (A, B, C, D). Wells without a Cell Seeding Stopper served as the positive control.

3.7. Assessment of endothelial biomarkers in the matrigel-grown MRC-5 cell cultures

To further verify at the molecular level, the macroscopic observation of endothelial-like tube formation of MRC-5 cells grown on matrigel, additional experiments were carried out to assess the gene expression level of seven specific endothelial biomarker genes. The selected genes were *Kinase Insert Domain Receptor* (KDR), *Purinergic Receptor* P2X 4 (P2RX4), *Cadherin 5* (CDH5), Cadherin 1 (CDH1), *Epithelial Cellular Adhesion Molecule* (EPCAM), *Angiotensin II Receptor Type 1* (AGTR1), and *Prostaglandin E Synthase* (PTGES) [32]. Notably, we included in this experimentation the well-established endothelial model of the human umbilical vein endothelial cell line (HUVEC cells) to ensure the obtained data [24,27,32]. Initially, the MRC-5 and HUVEC cells ($1.5 × 10^{-5}$ cells/ml) were plated on 5mg/ml matrigel and allowed to grow in cultures for 24 hours. Interestingly, MRC-5 cells exhibited the sprouting morphology (Figure 8A, B, C), whereas HUVEC cells showed the typical endothelial tube-formation structures (Figure 8D, E, F). Also, cultures of MRC-5 and HUVEC cells grown in 24 well-plates without matrigel served as a control for comparative evaluation of the data. As shown in Figure 8H, the gene expression level of all the seven endothelial biomarkers studied in matrigel-plated HUVEC cells has shown a statistically significant increase after 24hr incubation, as expected [24]. Similarly, MRC-5 cells grown on matrigel and subjected to the same conditions as HUVEC ones also presented higher levels of all seven endothelial biomarkers (Figure 8G), although not comparable to HUVEC cells' behavior, as shown in Figure 8I. By further evaluating the data taken from MRC-5 cells grown on matrigel, it is obvious that out of the seven endothelial biomarkers studied, three of them, KDR, P2RX4 and CDH5, have presented a higher increase in their gene expression. Based on this observation, an additional and complementary experiment was carried out in which the MRC-5 cell cultures were allowed to grow on a higher matrigel concentration (10 mg/ml) for a 24-48hr period in cultures before to assess again the gene expression level of these biomarkers. According to the results indicated in Figure 9G), the expression levels of KDR, P2RX4 and CDH5 genes did not exhibit substantial alterations following a 48hr incubation with matrigel 10mg/ml compared to the changes seen in MRC-5 cells plated on matrigel 5mg/ml (Figure 8G). However, between the three genes, the expression level of CDH5 has shown a higher increase in gene expression (Figure 9G).   Noticeably again, MRC-5 cells grown on the higher matrigel concentration (10mg/ml) now exhibited the tube-formation structures even from the 24hr period of incubation. Overall, these data confirm that MRC-5 cells grown on matrigel form the tubular structures in a manner that the expression of endothelial biomarker genes increases although to a much lower level than that seen in the endothelial model system of HUVEC cells may be due to their different histological and developmental nature. Further work is needed to investigate any potential clinical exploitation of such observations within the concept of regenerative medicine.
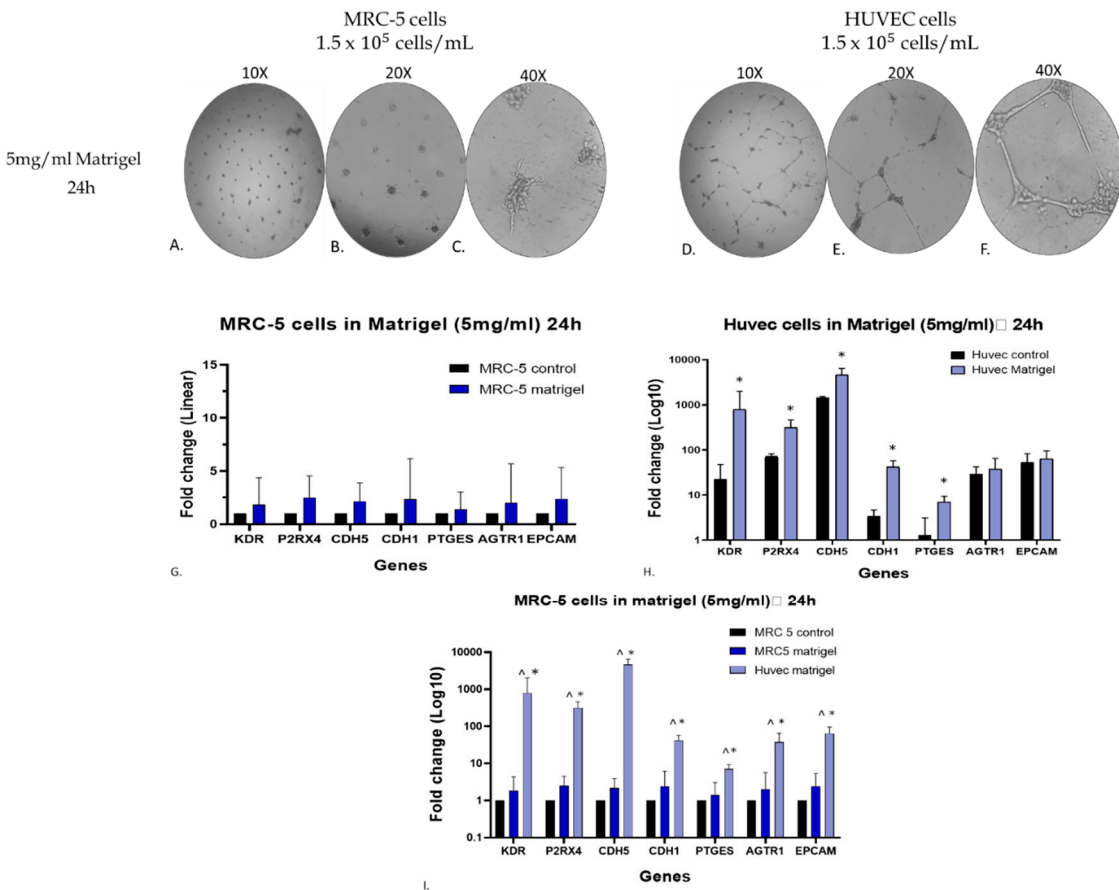
Figure 8. Assessment of gene expression level of endothelial biomarkers by qPCR analysis. MRC-5 (A, B, C) and HUVEC (D, E, F) cells were grown on matrigel (5mg/ml) for 24 hours, whereas as control cultures were used MRC-5 and/or HUVEC cells grown in plates without matrigel. Due to the different levels of expression between MRC-5 and HUVEC cells, the expression level of each gene is depicted either as linear fold increase for MRC-5 (G) or logarithmic fold change for HUVEC (H) +/- standard deviation (n=3-5). Notably, these obtained gene expression data from MRC-5 and HUVEC cells are also shown in the panel I to allow the comparison between the two cell lines. The * symbolizes the statistically significant differences in the expression level of each gene between the control group and the matrigel-grown cell cultures.
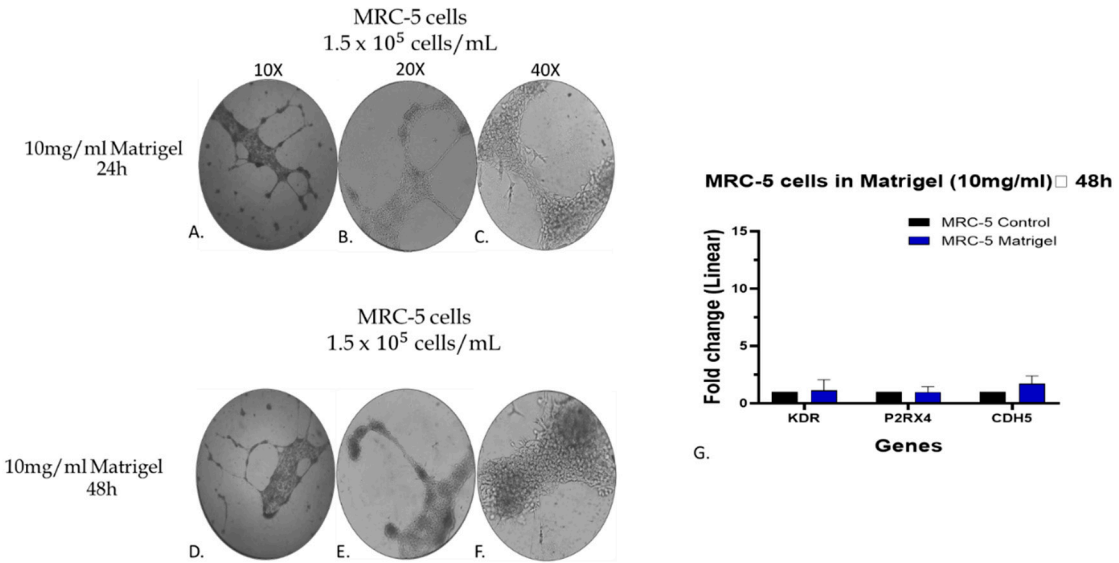
Figure 9. Assessment of the gene expression level of KDR, P2RX4 and CDH5 endothelial biomarkers by qPCR analysis in MRC-5 cells grown on matrigel 10mg/ml. The morphology of cells grown for 24 (A, B, C) and/or 48 hrs (D, E, F) is shown. As control culture was used MRC-5 cells grown in plates without matrigel. In panel G, the expression level of each gene is depicted as fold change +/- standard deviation (n=3-5).

4. Discussion

The present study aimed to clarify whether human lung FBs can differentiate into an endothelial-like cell type. Differentiation was evaluated by the formation of capillary-like networks on top of the thick gel of Matrigel and also the alignment of capillary sprouts to form complex three-dimensional networks of new blood vessels. Our data support the hypothesis that MRC-5 cells have the potential to tubulogenesis expressing endothelial biomarkers upon culture on Matrigel and that cell density influences the capacity of tube formation *in vitro*. These results imply that the microenvironment and cell-cell interactions clearly contribute to MRC-5 cell decisions. As a matter of fact, an increase in fibroblast density might reasonably be expected to promote angiogenesis, a fact that have to be taken into consideration in potential clinical applications. The presented herein results are in line with similar observations reported for *in vivo* differentiation of FBs. [33]

Previous studies have shown that fibroblasts can serve as a source of angiogenic mediators, such as vascular endothelial growth factor, which induce EC sprouting, are required for EC lumen formation, and thus play an important role in tumor angiogenesis. [17,18] In addition, fibroblasts significantly contribute to angiogenesis by directly converting to endothelial cells through mesenchymal to endothelial transition. Cardiac fibroblasts were reported to contribute to cardiac neovascularization by converting to endothelial cells through mesenchymal to endothelial transition (MEndoT) after cardiac injury which may represent a therapeutic target for enhancing vascularity and repair of ischemic tissues.[25] Moreover, Meng et al reported that a subpopulation of interstitial cells with fibroblast-like features contributes to angiogenesis and improves recovery of ischemic skeletal muscle by converting to endothelial cells. [22] while in two separate previous studies, it was reported that both human and mouse fibroblasts can be directly converted to endothelial cells by defined factors. [20,21,34]

Nevertheless, the present study provides a novel insight into the phenomenon of angiogenesis. The results obtained in the present study showed that fibroblasts differentiated toward an endothelial cell-like phenotype were successfully cultured on top of and embedded in the Matrigel scaffold. The matrix has previously been used in numerous *in vitro* and *in vivo* studies, exhibiting interesting results regarding cell viability, migration, and proliferation. Our results are in line with these previous findings. MRC-5 cells went through several passages before the start of experiments, thus preventing ECs from the original tissue sample to attach and proliferate. The use of several distinct single-cell clones also greatly reduces the risk of false positives as a result of contamination.

Several innovations in fibroblast differentiation strategies are presented herein. Firstly, it is demonstrated for first time that MRC-5 human lung fibroblasts can be directly converted to ECs. In previous studies, the conditioned medium (CM) from MRC-5 fibroblasts cells, induced HUVECs to form much more tube-like structures compared to the Nor-CM group [35] or endothelial colony-forming cells (ECFCs) to form new tubes and networks compared to those in unconditioned medium[36], on top of matrigel gel. Secondly, it was identified that MRC-5 cells were converted directly into endothelial cells after being cultured in fetal bovine serum without being previously cultured in Endothelial Growth Medium. In a previous related study endothelial differentiation of human dermal fibroblasts was induced by culturing cells in 30% human serum, but not in fetal calf serum. The formation of capillary-like networks was studied after FBs were cultured in Endothelial Growth Medium (EGM) for 10 days before being seeded onto gels.[24,37]. We further demonstrated that by growing MRC-5 cells on top of Matrigel hydrogel, the differentiated ECs exhibited the capability to form capillary structure within 24 h, or EC sprouts when being embedded in the matrix. MRC-5 cells have hereby exhibited an ability to build anastomotic tubular networks, on top of Matrigel gel both 24 and 48 h after seeding. Capillary sprouts originating from the spheroids gave

rise to complex anastomosing capillary-like networks similar to the ones reported by Korff T et al.[38], while HSC-3 spheroids embedded in Matrigel gel, under the same conditions, didn't give rise to sprouts, for at least 48 h after spheroid formation (Figure S1). VEGF, contained in Matrigel, profoundly increases sprouting, as no sprouts are observed in growth factor–deficient conditions, when MRC-5 spheroids are embedded in PuraMatrix Peptide Hydrogel which is a synthetic matrix used to create defined three-dimensional (3D) microenvironments for a variety of cell culture experiments. (Figure S2). Finally, invasion is generally perceived to be a late event during the progression of human cancer and previous research has shown that cancer-associated fibroblasts (CAFs) induce invasion of cancer cells through the remodelling of the ECM.[39] However, in the current study, it was tested for the first time, not the ability of MRC-5 cells to induce invasion of cancer cells, but the ability of these specific cells to invade the gel.

In summary, this is the first study to our knowledge to demonstrate that MRC-5 lung fibroblasts can be directly converted to ECs. This ability firstly demonstrated here, therefore sheds new light on endothelial differentiation and reprogramming and constitutes significant progress toward future clinical applications. This direct conversion of lung fibroblasts into ECs can provide new therapeutic modalities to overcome the obstacles of the past associated with the clinical application of embryonic stem cell– or iPSC-derived ECs. Moreover, induced lung FBs may function as a new cell source for the formation of vascular networks in engineered three-dimensional tissues *in vitro* and facilitate the creation of tissue-engineered grafts. Such evidence provides new insights on the way to therapeutically exploit normal human fibroblasts in clinical conditions, since MRC-5 cells are already used in the production of human vaccines ([40,41]), by simply culturing them *in vitro* in well-defined matrices that could be accepted for such applications by the drug regulatory bodies. Further research, however, is yet to be done to establish the precise mechanisms which act on MRC-5 human fibroblasts to transform them into ECs.

5. Conclusions

The current work presents for first-time evidence that human MRC-5 lung FBs can alter their phenotype towards an EC-like phenotype by culturing them on Matrigel matrices. This fact is interesting, since MRC-5 cells are already used in the production of vaccines for human immunization under the conditions of strict rules of the regulatory environment, so the potential *in vitro* differentiation of FBs into EC-like cells may lead to new regimens for treating diseases, where tissues lack sufficient blood supply and endogenous angiogenesis is inadequate.

References

1. Meinhart, J.G.; Deutsch, M.; Fischlein, T.; Howanietz, N.; Fröschl, A.; Zilla, P. Clinical Autologous in Vitro Endothelialization of 153 Infrainguinal EPTFE Grafts. *Annals of Thoracic Surgery* **2001**, *71*, S327–S331, doi:10.1016/S0003-4975(01)02555-3.

2. Baguneid, M.S.; Seifalian, A.M.; Salacinski, H.J.; Murray, D.; Hamilton, G.; Walker, M.G. Tissue Engineering of Blood Vessels. *British Journal of Surgery* **2006**, *93*, 282–290, doi:10.1002/bjs.5256.

3. L'heureux, N.; Pâquet, S.; Labbé, R.; Germain, L.; Auger, F.A. A Completely Biological Tissue-Engineered Human Blood Vessel. *The FASEB Journal* **1998**, *12*, 47–56, doi:10.1096/fasebj.12.1.47.

4. Bergmeister, H.; Strobl, M.; Grasl, C.; Liska, R.; Schima, H. Tissue Engineering of Vascular Grafts. *European Surgery - Acta Chirurgica Austriaca* **2013**, *45*, 187–193, doi:10.1007/s10353-013-0224-x.

5. Weinberg, C.B.; Bell, E. A Blood Vessel Model Constructed from Collagen and Cultured Vascular Cells. *Science* **1986**, *231*, 397–400, doi:10.1126/science.2934816.

6. Conte, M.S. Critical Appraisal of Surgical Revascularization for Critical Limb Ischemia. *J Vasc Surg* **2013**, *57*, 8S-13S, doi:10.1016/j.jvs.2012.05.114.

7. Chew, D.K.W.; Owens, C.D.; Belkin, M.; Donaldson, M.C.; Whittemore, A.D.; Mannick, J.A.; Conte, M.S. Bypass in the Absence of Ipsilateral Greater Saphenous Vein: Safety and Superiority of the Contralateral Greater Saphenous Vein. *J Vasc Surg* **2002**, *35*, 1085–1092, doi:10.1067/mva.2002.124628.

8. Klinkert, P.; Post, P.N.; Breslau, P.J.; van Bockel, J.H. Saphenous Vein versus PTFE for Above-Knee Femoropopliteal Bypass. A Review of the Literature. *European Journal of Vascular and Endovascular Surgery* **2004**, *27*, 357–362, doi:10.1016/j.ejvs.2003.12.027.

9. Timmermans, F.; Plum, J.; Yöder, M.C.; Ingram, D.A.; Vandekerckhove, B.; Case, J. Endothelial Progenitor Cells: Identity Defined? *J Cell Mol Med* **2009**, *13*, 87–102, doi:10.1111/j.1582-4934.2008.00598.x.

10. Asahara, T.; Murohara, T.; Sullivan, A.; Silver, M.; van der Zee, R.; Li, T.; Witzenbichler, B.; Schatteman, G.; Isner, J.M. Isolation of Putative Progenitor Endothelial Cells for Angiogenesis. *Science (1979)* **1997**, *275*, 964–967, doi:10.1126/science.275.5302.964.

11. Moore, K.A.; Lemischka, I.R. Stem Cells and Their Niches. *Science (1979)* **2006**, *311*, 1880–1885, doi:10.1126/science.1110542.

12. Zuk, P.A.; Zhu, M.; Mizuno, H.; Huang, J.; Futrell, J.W.; Katz, A.J.; Benhaim, P.; Lorenz, H.P.; Hedrick, M.H. Multilineage Cells from Human Adipose Tissue: Implications for Cell-Based Therapies. *Tissue Eng* **2001**, *7*, 211–228, doi:10.1089/107632701300062859.

13. Pittenger, M.F.; Mackay, A.M.; Beck, S.C.; Jaiswal, R.K.; Douglas, R.; Mosca, J.D.; Moorman, M.A.; Simonetti, D.W.; Craig, S.; Marshak, D.R. Multilineage Potential of Adult Human Mesenchymal Stem Cells. *Science (1979)* **1999**, *284*, 143–147, doi:10.1126/science.284.5411.143.

14. Abbas, O.L.; Özatik, O.; Gönen, Z.B.; Öğüt, S.; Özatik, F.Y.; Salkın, H.; Musmul, A. Comparative Analysis of Mesenchymal Stem Cells from Bone Marrow, Adipose Tissue, and Dental Pulp as Sources of Cell Therapy for Zone of Stasis Burns. *Journal of Investigative Surgery* **2019**, *32*, 477–490, doi:10.1080/08941939.2018.1433254.

15. Humphrey, J.D.; Dufresne, E.R.; Schwartz, M.A. Mechanotransduction and Extracellular Matrix Homeostasis. *Nat Rev Mol Cell Biol* **2014**, *15*, 802–812, doi:10.1038/nrm3896.

16. Watt, F.M.; Fujiwara, H. Cell-Extracellular Matrix Interactions in Normal and Diseased Skin. *Cold Spring Harb Perspect Biol* **2011**, *3*, 1–14, doi:10.1101/cshperspect.a005124.

17. Newman, A.C.; Nakatsu, M.N.; Chou, W.; Gershon, P.D.; Hughes, C.C.W. The Requirement for Fibroblasts in Angiogenesis: Fibroblast-Derived Matrix Proteins Are Essential for Endothelial Cell Lumen Formation. *Mol Biol Cell* **2011**, *22*, 3791–3800, doi:10.1091/mbc.E11-05-0393.

18. Ito, T.K.; Ishii, G.; Chiba, H.; Ochiai, A. The VEGF Angiogenic Switch of Fibroblasts Is Regulated by MMP-7 from Cancer Cells. *Oncogene* **2007**, *26*, 7194–7203, doi:10.1038/sj.onc.1210535.

19. Ginsberg, M.; James, D.; Ding, B. sen; Nolan, D.; Geng, F.; Butler, J.M.; Schachterle, W.; Pulijaal, V.R.; Mathew, S.; Chasen, S.T.; et al. Efficient Direct Reprogramming of Mature Amniotic Cells into Endothelial Cells by ETS Factors and TGFβ Suppression. *Cell* **2012**, *151*, 559–575, doi:10.1016/j.cell.2012.09.032.

20. Lee, S.; Park, C.; Han, J.W.; Kim, J.Y.; Cho, K.; Kim, E.J.; Kim, S.; Lee, S.J.; Oh, S.Y.; Tanaka, Y.; et al. Direct Reprogramming of Human Dermal Fibroblasts into Endothelial Cells Using ER71/ETV2. *Circ Res* **2017**, *120*, 848–861, doi:10.1161/CIRCRESAHA.116.309833.

21. Han, J.K.; Chang, S.H.; Cho, H.J.; Choi, S.B.; Ahn, H.S.; Lee, J.; Jeong, H.; Youn, S.W.; Lee, H.J.; Kwon, Y.W.; et al. Direct Conversion of Adult Skin Fibroblasts to Endothelial Cells by Defined Factors. *Circulation* **2014**, *130*, 1168–1178, doi:10.1161/CIRCULATIONAHA.113.007727.

22. Meng, S.; Lv, J.; Chanda, P.K.; Owusu, I.; Chen, K.; Cooke, J.P. Reservoir of Fibroblasts Promotes Recovery from Limb Ischemia. *Circulation* **2020**, 1647–1662, doi:10.1161/CIRCULATIONAHA.120.046872.

23. Roy, B.; Yuan, L.; Lee, Y.; Bharti, A.; Mitra, A.; Shivashankar, G. v. Fibroblast Rejuvenation by Mechanical Reprogramming and Redifferentiation. *Proc Natl Acad Sci U S A* **2020**, *117*, 10131–10141, doi:10.1073/pnas.1911497117.

24. Junker, J.P.E.; Lönnqvist, S.; Rakar, J.; Karlsson, L.K.; Grenegård, M.; Kratz, G. Differentiation of Human Dermal Fibroblasts towards Endothelial Cells. *Differentiation* **2013**, *85*, 67–77, doi:10.1016/j.diff.2013.01.005.

25. Ubil, E.; Duan, J.; Pillai, I.C.L.; Rosa-Garrido, M.; Wu, Y.; Bargiacchi, F.; Lu, Y.; Stanbouly, S.; Huang, J.; Rojas, M.; et al. Mesenchymal–Endothelial Transition Contributes to Cardiac Neovascularization. *Nature 2014 514:7524* **2014**, *514*, 585–590, doi:10.1038/nature13839.

26. Tseligka, E.D.; Rova, A.; Amanatiadou, E.P.; Calabrese, G.; Tsibouklis, J.; Fatouros, D.G.; Vizirianakis, I.S. Pharmacological Development of Target-Specific Delocalized Lipophilic Cation-Functionalized Carboranes for Cancer Therapy. *Pharm Res* **2016**, *33*, 1945–1958, doi:10.1007/s11095-016-1930-4.

27. Medina-Leyte, D.J.; Domínguez-Pérez, M.; Mercado, I.; Villarreal-Molina, M.T.; Jacobo-Albavera, L. Use of Human Umbilical Vein Endothelial Cells (HUVEC) as a Model to Study Cardiovascular Disease: A Review. *Applied Sciences* **2020**, *10*, doi:10.3390/APP10030938.

28. Islam, S.; Flaherty, P. Assay Methods Protocol: Endothelial Cell Tube Formation Assay. *Corning Incorporated* **2013**, 2–5.

29. Corporation, P. Total RNA Isolation from 3D Cell Cultures or Cells in Matrigel ® Matrix Using the ReliaPrep ™ MiRNA Cell and Tissue Miniprep System Disclaimers : 18–19.

30. Carpentier, G.; Berndt, S.; Ferratge, S.; Rasband, W.; Cuendet, M.; Uzan, G.; Albanese, P. Angiogenesis Analyzer for ImageJ — A Comparative Morphometric Analysis of "Endothelial Tube Formation Assay" and "Fibrin Bead Assay." *Sci Rep* **2020**, *10*, 1–13, doi:10.1038/s41598-020-67289-8.

31. Tevis, K.M.; Colson, Y.L.; Grinstaff, M.W. Embedded Spheroids as Models of the Cancer Microenvironment. *Adv Biosyst* **2017**, *1*, doi:10.1002/adbi.201700083.

32. Kumar, R.; Harris-Hooker, S.; Kumar, R.; Sanford, G. Co-Culture of Retinal and Endothelial Cells Results in the Modulation of Genes Critical to Retinal Neovascularization. *Vasc Cell* **2011**, *3*, 27, doi:10.1186/2045-824X-3-27.

33. Kon, K.; Fujiwara, T. Transformation of Fibroblasts into Endothelial Cells during Angiogenesis. *Cell Tissue Res* **1994**, *278*, 625–628, doi:10.1007/BF00331383.

34. Li, J.; Huang, N.F.; Zou, J.; Laurent, T.J.; Lee, J.C.; Okogbaa, J.; Cooke, J.P.; Ding, S. Conversion of Human Fibroblasts to Functional Endothelial Cells by Defined Factors. *Arterioscler Thromb Vasc Biol* **2013**, *33*, 1366–1375, doi:10.1161/ATVBAHA.112.301167.

35. Zhou, L.; Sun, L.; Lin, S.; Fang, D.; Zhao, R.; Zhu, J.; Liu, J.; Chen, L.; Shi, W.; Yuan, S.; et al. Inhibition of Angiogenic Activity of Hypoxic Fibroblast Cell Line MRC-5 in Vitro by Topotecan. *Medical Oncology* **2011**, *28*, 653–659, doi:10.1007/s12032-010-9710-1.

36. Menicacci, B.; Margheri, F.; Laurenzana, A.; Chillà, A.; del Rosso, M.; Giovannelli, L.; Fibbi, G.; Mocali, A. Chronic Resveratrol Treatment Reduces the Proangiogenic Effect of Human Fibroblast "Senescent-Associated Secretory Phenotype" on Endothelial Colony-Forming Cells: The Role of IL8. *Journals of Gerontology - Series A Biological Sciences and Medical Sciences* **2019**, *74*, 625–633, doi:10.1093/gerona/gly175.

37. Karlsson, L.K.; Junker, J.P.E.; Grenegård, M.; Kratz, G. Human Dermal Fibroblasts: A Potential Cell Source for Endothelialization of Vascular Grafts. *Ann Vasc Surg* **2009**, *23*, 663–674, doi:10.1016/j.avsg.2009.03.007.

38. Korff, T.; Augustin, H.G. Tensional Forces in Fibrillar Extracellular Matrices Control Directional Capillary Sprouting. *J Cell Sci* **1999**, *112*, 3249–3258, doi:10.1242/jcs.112.19.3249.

39. Attieh, Y.; Clark, A.G.; Grass, C.; Richon, S.; Pocard, M.; Mariani, P.; Elkhatib, N.; Betz, T.; Gurchenkov, B.; Vignjevic, D.M. Cancer-Associated Fibroblasts Lead Tumor Invasion through Integrin-B3-Dependent Fibronectin Asse. *Journal of Cell Biology* **2017**, *216*, 3509–3520, doi:10.1083/jcb.201702033.

40. Zhang, K.; Na, T.; Wang, L.; Gao, Q.; Yin, W.; Wang, J.; Yuan, B.Z. Human Diploid MRC-5 Cells Exhibit Several Critical Properties of Human Umbilical Cord-Derived Mesenchymal Stem Cells. *Vaccine* **2014**, *32*, 6820–6827, doi:10.1016/j.vaccine.2014.07.071.

41.   World Health Organization WHO Expert Committee on Biological Standardization, Annex 3: Reccomendations for the Evaluation of Animal Cell Cultures as Substrates for the Manufacture of Biological Medicinal Products and for the Characterization of Cell Banks. *World Health Organ Tech Rep Ser* **2013**, 79–187.